J. KSIAM Vol.2, No.2, 97-109, 1998

A Heat Loss Comparison Between the Two Parabolic Fin Models Using Two Different Numerical Methods

K.T.Kim*, H.S.Kang**
* : Graduate School, Kangwon University
** : Department of Mechanical Engineering, Kangwon University

Abstract

A comparison of the two dimensional heat loss, computed using the analytical method and the finite difference method in two models(i.e. one is a parabolic fin whose parabolic curves meet at the fin center line and the other is a transformed parabolic fin whose tip cuts vertically), is made assuming the analytical method is correct. For these methods, the root temperature and surrounding convection coefficients of these fins are assumed as constants. The results show that the relative errors of the heat loss between the two methods for the parabolic fin whose tip cuts vertically are smaller than those for the one whose tip does not cut. In case of Bi=0.01, the values of the heat loss obtained using a finite difference method are close to those values obtained using the analytical method for both models. The values of the heat loss from both models calculated by using the analytical method are almost the same for given range of non-dimensional fin length in case of Bi = 0.01 and 0.1.

1. Introduction

There are many papers dealing with the fin so far. Many papers analyze the fin itself while some papers present the performance improvement of the machine by attaching the fin [1, 2] to the machine. It has been shown that the one-dimensional approach [3, 4, 5], is convenient, but may be in error for certain physical conditions. Various shapes of the fin (i.e. rectangular [4 7, 8], triangular [8, 11], trapezoidal [3, 11] and annular [12, 13] etc.) have been studied. No literature seems to be available which presents the analysis of a two dimensional parabolic fin by analytical method. The problem seems to be due to the difficulty in appling the boundary conditions to the fin.

This study performed two-dimensional analyses on the parabolic fins by using two different numerical methods. One is the analytical method and the other is a finite difference method. For parabolic fins, two models are chosen. The shape of model 1 is a parabolic fin whose parabolic curves meet at the fin center line and that of model

Key Words : Parabolic Fin, Heat Loss, Relative Error.

2 is a transformed parabolic fin whose fin tip cuts vertically. For the finite difference methods, 55 nodes for model 1 and 57 nodes for model 2 in the upper half of the fin was convenient. That is, checks run for several different configurations (number of nodes) indicated that these nodes were sufficient for the solutions to be consistent. Further, for this setup, the non-dimensional fin length is restricted to be less than 3 in order to prevent any error which might result due to Δx being too large as the non-dimensional fin length increases. Also, the non-dimensional fin length was restricted to be less than 6 in order to decrease errors due to the number of iteration in case of the analytical method. Each analysis was based on the following assumptions: the root temperature, surrounding convection coefficient and fin thermal conductivity are constants and the condition is steady-state.

2. Two-Dimensional Numerical Analysis

2.1 Analytical Method

Based upon the fins illustrated in Fig. 1-a and Fig. 1-b, the two dimensional analysis is governed by the form of the 1st Law of thermodynamics shown as Eq. (1).

$$\frac{\partial^2\theta}{\partial x^2} + \frac{\partial^2\theta}{\partial y^2} = 0 \tag{1}$$

Three boundary conditions are represented as Eqs. (2) (4) for both models and one energy balance equation is shown as Eq. (5) for model 1 and Eq. (6) for model 2.

$$\theta = \theta_0 \quad at \quad x = 0 \tag{2}$$

$$\frac{\partial\theta}{\partial x} + Bi \cdot \theta = 0 \quad \begin{cases} at \quad x = L & \text{for model 1} \\ at \quad x = LL & \text{for model 2} \end{cases} \tag{3}$$

$$\frac{\partial\theta}{\partial y} = 0 \quad at \quad y = 0 \tag{4}$$

$$-\int_0^1 \frac{\partial\theta}{\partial x}\bigg|_{x=0} dy = Bi \cdot \int_0^1 \theta \cdot \sqrt{\frac{L^2}{4y} + 1}\, dy \tag{5}$$

$$-\int_0^1 \frac{\partial\theta}{\partial x}\bigg|_{x=0} dy = Bi \cdot \int_{0.05}^1 \theta \cdot \sqrt{\frac{L^2}{4y} + 1}\, dy - \int_0^{0.05} \frac{\partial\theta}{\partial x}\bigg|_{x=LL} dy \tag{6}$$

where,

$$x = \frac{x'}{l}, \quad y = \frac{y'}{l}, \quad L = \frac{L'}{l}, \quad LL = 0.776393L, \quad Bi = \frac{h \cdot l}{k},$$
$$\theta = T - T_\infty, \text{ and } \theta_0 = T_w - T_\infty$$

The value of LL is chosen arbitrary. From Eq. (1) with three boundary conditions and one energy balance equation, the temperature profile can be obtained by the usual separation of variables procedure. The result is

$$\theta = \sum_{n=1}^{\infty} \theta_0 \cdot N_n \cdot f_n(x) \cdot f_n(y) \tag{7}$$

where,

$$N_n = \frac{4\theta_0 \cdot \sin\lambda_n}{2\lambda_n + \sin(2\lambda_n)} \tag{8}$$

$$f_n(x) = \frac{\lambda_n \cdot \cosh A_n + Bi \cdot \sinh A_n}{\lambda_n \cdot \cosh C_n + Bi \cdot \sinh C_n} \tag{9}$$

$$f_n(y) = \cos(\lambda_n \cdot y) \tag{10}$$

In Eq. (9) $A_n = \lambda_n(L - x)$, $C_n = \lambda_n \cdot L$ for model 1 and $A_n = \lambda_n(LL - x)$, $C_n = \lambda_n \cdot LL$ for model 2. Eigenvalues for model 1 are obtained by using Eq. (11) derived from Eq. (3) and Eq. (5).

$$\begin{aligned}[\lambda_n \cdot \sinh C_n + Bi \cdot \cosh C_n] \cdot \sin(\lambda_n) = {} & 2 \cdot A \sum_{i=1}^{\infty}\sum_{j=1}^{\infty} A_{i,j} \cdot \lambda_n^{2i+2j-3} \\ & - A \sum_{i=1}^{\infty}\sum_{j=1}^{\infty}\sum_{k=1}^{i+2j-2} A_{i,j} \cdot C_{i,j} \cdot D_{i,j,k} \cdot \lambda_n^{2i+2j-3} + C \sum_{i=1}^{\infty}\sum_{j=1}^{\infty} A_{i,j} \cdot E_{i,j} \cdot \lambda_n^{2i+2j-3} \\ & + Bi^2 \times \sum_{i=1}^{\infty}\sum_{j=1}^{\infty}\sum_{k=1}^{i+2j-2} F_{i,j} \cdot (G_{i,j,k} - H_{i,j,k}) \cdot \lambda_n^{2i+2j-3}\end{aligned} \tag{11}$$

where,

$$A = Bi \cdot \sqrt{\frac{L^2}{4} + 1} \tag{12}$$

$$C = Bi \cdot \ln\left[\frac{\sqrt{\frac{L^2}{4} + 1} - 1}{\sqrt{\frac{L^2}{4} + 1} + 1}\right] \tag{13}$$

$$A_{i,j} = \frac{(-1)^{j-1} \cdot L^{2i-2}}{\Gamma(2i-1) \cdot \Gamma(2j-1) \cdot (2i+4j-5)} \tag{14}$$

$$C_{i,j} = \frac{L^{2i+4j-4} \cdot \Gamma(2i+4j-3)}{4^{i+2j-2} \cdot [\Gamma(i+2j-1)]^2} \tag{15}$$

$$D_{i,j,k} = \frac{\Gamma(k+1) \cdot \Gamma(k)}{(-4)^{i+2j-k-2} \cdot \Gamma(2k+1) \cdot \left(\frac{L^2}{4}\right)^k} \tag{16}$$

$$E_{i,j} = \frac{L^{2i+4j-4} \cdot \Gamma(2i+4j-3)}{(-4)^{i+2j-2} \cdot [\Gamma(i+2j-1)]^2} \tag{17}$$

$$F_{i,j} = \frac{(-1)^{j-1} \cdot L^{2i-1} \cdot \Gamma(i+2j-2)}{\Gamma(2i) \cdot \Gamma(2j-1)} \tag{18}$$

$$G_{i,j,k} = \frac{2 \cdot \left(-\frac{L^2}{4}\right)^{i+2j-k-2} \cdot \left(\frac{L^2}{4} + 1\right)^{k+\frac{1}{2}}}{\Gamma(k) \cdot \Gamma(i+2j-k-1) \cdot (2k+1)} \tag{19}$$

$$H_{i,j,k} = \frac{\left(-\frac{L^2}{4}\right)^{i+2j-k-2} \cdot L \cdot \left(\frac{L^2}{4}\right)^k}{\Gamma(k) \cdot \Gamma(i+2j-k-1) \cdot (2k+1)} \tag{20}$$

Also, eigenvalues for model 2 can be obtained by using Eq. (21) derived from Eq. (3) and Eq. (6).

$$[\lambda_n \cdot \sinh C_n + Bi \cdot \cosh C_n] \cdot \sin(\lambda_n) - Bi \cdot \sin(0.05\lambda_n)$$
$$= AA_n \left[2 \cdot \sum_{i=1}^{\infty} \sum_{j=1}^{\infty} A_{i,j} \cdot L_{i,j} \cdot \lambda_n^{2i+2j-4} \right.$$
$$- \sum_{i=1}^{\infty} \sum_{j=1}^{\infty} \sum_{k=1}^{i+2j-2} A_{i,j} \cdot C_{i,j} \cdot D_{i,j,k} \cdot \lambda_n^{2i+2j-4} \cdot M_k$$
$$\left. + \left(\frac{C}{Bi} - D \right) \sum_{i=1}^{\infty} \sum_{j=1}^{\infty} A_{i,j} \cdot E_{i,j} \cdot \lambda_n^{2i+2j-3} \right]$$
$$+ 2 \cdot CC_n \times \sum_{i=1}^{\infty} \sum_{j=1}^{\infty} \sum_{k=1}^{i+2j-2} F_{i,j} \cdot (G_{i,j,k} - N_{i,j,k}) \cdot \lambda_n^{2i+2j-3} \quad (21)$$

where,

$$AA_n = Bi \cdot \lambda_n \cdot \cosh D_n - Bi^2 \cdot \sinh D_n \quad (22)$$

$$CC_n = Bi^2 \cdot \cosh D_n - Bi \cdot \lambda_n \cdot \sinh D_n \quad (23)$$

$$L_{i,j} = \sqrt{\frac{L^2}{4} + 1} - \frac{\sqrt{5L^2 + 1}}{20^{i+2j-2}} \quad (24)$$

$$M_k = \sqrt{\frac{L^2}{4} + 1} - \frac{\sqrt{5L^2 + 1}}{(20)^k} \quad (25)$$

$$D = \ln \frac{\sqrt{5L^2 + 1} - 1}{\sqrt{5L^2 + 1} + 1} \quad (26)$$

$$N_{i,j,k} = \frac{\left(-\frac{L^2}{4}\right)^{i+2j-k-2} \cdot \left(\frac{L^2}{4} + 0.05\right)^{k+\frac{1}{2}}}{\Gamma(k) \cdot \Gamma(i + 2j - k - 1) \cdot (2k + 1)} \quad (27)$$

$$D_n = \lambda_n \cdot (L - LL) \quad (28)$$

In Eqs. (14) (20) and Eq. (27), Γ is a gamma function. Finally the heat loss can be calculated by Eq. (29) for both models.

$$Q = \int_{-1}^{1} -k \cdot \left. \frac{\partial \theta}{\partial x} \right|_{x=0} \cdot dy = 2k \cdot \theta_0 \sum_{n=1}^{\infty} f_n \cdot N_n \cdot \sin(\lambda_n) \quad (29)$$

where,

$$f_n = \frac{Bi \cdot \cosh C_n + \lambda_n \cdot \sinh C_n}{\lambda_n \cdot \cosh C_n + Bi \cdot \sinh C_n} \quad (30)$$

2.2 Finite Difference Method

For this method, 55 nodes were used for the upper half part of the model 1 (see Fig. 2-a) and the equations for each node are shown as Eq. (31) through Eq. (37).

For node 1(11, 20, 28, 35, 41, 46, 50)

$$\theta_0 - [1 + f_1 \cdot (f_1 + f_2) + g_{1,2}] \cdot \theta_1 + [f_1 \cdot (f_1 + f_2)] \cdot \theta_2 + g_{1,2} \cdot \theta_{11} = 0 \quad (31)$$

For node 2(and a similar form for the other interior points - 3, 12 and so on)

$$\theta_0 + \frac{1}{2} \cdot [f_1 \cdot (f_1 + f_2)] \cdot \theta_1 - [1 + f_1 \cdot (f_1 + f_2) + g_{1,2}] \cdot \theta_2$$

$$+ \frac{1}{2} \cdot [f_1 \cdot (f_1 + f_2)] \cdot \theta_3 + g_{1,2} \cdot \theta_{12} = 0 \quad (32)$$

For node 9(18, 26, 33, 39, 44, 48)

$$\theta_0 + [(f_1 + f_2) \cdot RA_{1,2}] \cdot \theta_8 - [1 + 2 \cdot (f_1 + f_2) \cdot RA_{1,2} + g_{1,2}] \cdot \theta_9 + [(f_1 + f_2) \cdot RA_{1,2}] \cdot \theta_{10} + g_{1,2} \cdot \theta_{19} = 0 \quad (33)$$

For node 10(19, 27, 34, 40, 45, 49, 52)

$$\theta_0 + (f_1 \cdot RB_{1,2}) \cdot \theta_9 - \left[1 + (f_1 \cdot RB_{1,2}) + Bi \cdot \Delta x_1 \cdot \sqrt{(RB_{1,2})^2 + 1}\right] \cdot \theta_{10} = 0 \quad (34)$$

For node 53

$$\theta_{50} - [1 + f_9 \cdot SA + g_{9,10}] \cdot \theta_{53} + (f_9 \cdot SA) \cdot \theta_{54} + g_{9,10} \cdot \theta_{55} = 0 \quad (35)$$

For node 54

$$\theta_{51} + [f_9 \cdot SB] \cdot \theta_{53} - \left[1 + f_9 \cdot SB + Bi \cdot \Delta x_9 \cdot \sqrt{SB^2 + 1}\right] \cdot \theta_{54} = 0 \quad (36)$$

For node 55

$$\theta_{53} - \left[1 + Bi \cdot \Delta x_{10} \times \sqrt{4 \cdot \left(\frac{\Delta x_{10} - Z}{\Delta y}\right)^2 + 1}\right] \cdot \theta_{55} = 0 \quad (37)$$

where,

$$f_i = \frac{\Delta x_i}{\Delta y}, \quad g_{i,j} = \frac{\Delta x_i}{\Delta x_j}, \quad RA_{i,j} = \frac{\Delta x_i}{\Delta y + \Delta y_j}, \quad RB_{i,j} = \frac{\Delta x_i + \Delta x_j}{2\Delta y + \Delta y_i - \Delta y_j}$$

$$Z \cong 0.293L, \quad SA = \frac{\Delta x_9 + 2Z}{\Delta y}, \text{ and } SB = \frac{\Delta x_9 + 2Z}{\Delta y + \Delta y_9}$$

In case of the model 2, 57 nodes were used for the upper half part (see Fig. 2-b) and the equations for each node are shown as Eq. (38) through Eq. (47). To obtain the value of the temperature of each node for both models, Gaussian elimination method is used.

For node 1(11,20,28,35,41,46)

$$\theta_0 - [1 + (f_1 + f_2) \cdot t_{1,10,11} + g_{1,2}] \cdot \theta_1 + [(f_1 + f_2) \cdot t_{1,10,11}] \cdot \theta_2 + g_{1,2} \cdot \theta_{11} = 0 \quad (38)$$

For node 2(12,21,29,36,42,47,51)

$$\theta_0 + [(f_1 + f_2) \cdot u_{1,9,10,11}] \cdot \theta_1 - [1 + 2 \cdot (f_1 + f_2) \cdot u_{1,9,10,11} + g_{1,2}] \cdot \theta_2 + [(f_1 + f_2) \cdot u_{1,9,10,11}] \cdot \theta_3 + g_{1,2} \cdot \theta_{12} = 0 \quad (39)$$

For node 3(and a similar form for the other interior points - 3, 12 and so on)

$$\theta_0 + [(f_1 + f_2) \cdot v_{1,8,9}] \cdot \theta_2 - [1 + 2 \cdot (f_1 + f_2) \cdot v_{1,8,9} + g_{1,2}] \cdot \theta_3 + [(f_1 + f_2) \cdot v_{1,8,9}] \cdot \theta_4 + g_{1,2} \cdot \theta_{13} = 0 \quad (40)$$

For node 10(19,27,34,40,45,49,52)

$$\theta_0 + [(f_1 + f_2) \cdot v_{1,1,2}] \cdot \theta_9$$

$$- \left[1 + (f_1 + f_2) \cdot v_{1,1,2} + Bi \cdot \Delta x_1 \cdot \sqrt{(RB_{1,2})^2 + 1}\right] \cdot \theta_{10} = 0 \qquad (41)$$

For node 50

$$\theta_{46} - \left[1 + (f_8 + f_9) \cdot VA_{8,10,11} + \frac{1}{2} \cdot (VB_{10,11} + VC_{10,11}) \cdot g_{8,9}\right] \cdot \theta_{50} + \left[(f_8 + f_9) \cdot VA_{8,10,11}\right] \cdot \theta_{51} + \frac{1}{2} \cdot g_{8,9} \cdot \left[VB_{10,11} \cdot \theta_{53} + VC_{10,11} \cdot \theta_{54}\right] = 0 \qquad (42)$$

For node 53

$$\theta_{50} - \left[1 + VD_{9,10,11} \cdot \frac{4\Delta x_9}{\Delta y_{11}} + g_{9,10}\right] \cdot \theta_{53} + \left[VD_{9,10,11} \cdot \frac{4\Delta x_9}{\Delta y_{11}}\right] \cdot \theta_{54} + g_{9,10} \cdot \theta_{56} = 0 \qquad (43)$$

For node 54

$$\theta_{50} + \left[VD_{9,10,11} \cdot VE_{9,10,11}\right] \cdot \theta_{53} - \left[1 + VD_{9,10,11} \cdot VE_{9,10,11} + VE_{9,10,11} \cdot VF_{9,10,11} + g_{9,10}\right] \cdot \theta_{54} + \left[VF_{9,10,11} \cdot VE_{9,10,11}\right] \cdot \theta_{55} + g_{9,10} \cdot \theta_{57} = 0 \qquad (44)$$

For node 55

$$\theta_{51} + \left[VF_{9,10,11} \cdot u_{9,9,10,11}\right] \cdot \theta_{54} - \left[1 + VF_{9,10,11} \cdot u_{9,9,10,11} + Bi \cdot \Delta x_9 \cdot \sqrt{(u_{9,9,10,11})^2 + 1}\right] \cdot \theta_{55} = 0 \qquad (45)$$

For node 56

$$\theta_{53} - \left[1 + 4 \cdot \left(\frac{\Delta x_{10}}{\Delta y_{11}}\right)^2 + Bi \cdot \Delta x_{10}\right] \cdot \theta_{56} + \left[4 \cdot \left(\frac{\Delta x_{10}}{\Delta y_{11}}\right)^2\right] \cdot \theta_{57} = 0 \qquad (46)$$

For node 57

$$\theta_{54} + \left[\frac{\Delta x_{10}}{\Delta y_{11}} \cdot VE_{10,11}\right] \cdot \theta_{56} - \left[1 + \frac{\Delta x_{10}}{\Delta y_{11}} \cdot VE_{10,11} + Bi \cdot \left(\frac{\Delta x_{10} \cdot \Delta y_{11}}{2\Delta y_{10} + \Delta y_{11}} + \frac{VE_{10,10,11}}{2} \times \sqrt{(\Delta x_{10})^2 + (\Delta y_{10})^2}\right)\right] \cdot \theta_{57} = 0 \qquad (47)$$

where,

$$t_{i,j,k} = \frac{\Delta x_i}{\Delta y_j + \Delta y_k}, \quad u_{i,j,k,l} = \frac{\Delta x_i}{2\Delta y + \Delta y_j - \Delta y_k - \Delta y_l}, \quad v_{i,j,k} = \frac{\Delta x_i}{2\Delta y + \Delta y_j - \Delta y_k}$$

$$VA_{i,j,k} = \frac{\Delta x_i}{\Delta y_j + \Delta y_k}, \quad VB_{i,j} = \frac{\Delta y_j}{\Delta y_j + \Delta y_j}, \quad VC_{i,j} = \frac{2\Delta y_i + \Delta y_j}{\Delta y_i + \Delta y_j},$$

$$, \; VD_{i,j,k} = \frac{\Delta x_i + \Delta x_j}{\Delta y_k}, \; VE_{i,j,k} = \frac{4\Delta x_i}{2\Delta y_j + \Delta y_k}, \text{ and } \; VF_{i,j,k} = \frac{\Delta x_i + \Delta x_j}{2\Delta y - \Delta y_k}$$

The definition of the values Δx_i, Δy_i (i = 1, 2) which are used in this finite difference method is shown in Fig. 2-c and the rest Δx_i, Δy_i (i = 3, 4, $\cdots$) can be written in the same procedure.

3. Results and Discussions

Figure 3 presents the relative error of the heat loss in the finite difference method as compared to the analytical method as L varies from 0.5 to 3.0 for several values of Biot number in case of the model 1. The relative error increases slowly and is less than 5 % for given range of L in case of Bi = 0.01. It is shown that the results become not so good as the value of Bi and L increase.

Results for the same conditions as in Fig. 3 except that the model 1 is changed to the model 2 are depicted in Fig. 4. The trend of the results are similar but the overall relative errors decrease considerably in comparison with Fig. 3. When Bi = 0.01, the relative error varies from 0.17 % to 1.26 % for given range of L. Also the relative error is less than 5 % for given range of L in case of Bi = 0.05 and for until L = 2 in case of Bi = 0.1. These improvement seem to be obtained by proper choosing the nodes for model 2.

Figure 5 shows the relative error of the heat loss in the finite difference method as compared to the analytical method as Biot number varies from 0.01 to 1.0 for L = 0.5, 1.0, 2.0 and 3.0 in case of the model 1. In the case of $L \leq 1.0$, the relative error increases regularly as the value of Biot number increases while it increases rapidly until Bi = 0.1 and varies somewhat irregularly in the range of $0.1 < Bi < 1.0$ for L = 2.0 and 3.0.

Figure 6 represents the same type of information as was presented as Fig. 5 but for model 2. For model 2, the relative errors increase somewhat regularly as Biot number increases for all values of L. The relative error for model 2 is less than that for model 1 overall and the relative error for L = 0.5 is less than 4 % for given range of Biot number. This figure shows that both two methods can be used for model 2 because Biot number is considered to be less than 0.1 in our usual circumstance.

Figure 7 shows the variation of the heat loss from the two fin models for $0.5 \leq L \leq 6.0$ and Bi = 0.01 when the analytical method was used. To compare the heat loss from the two fin models, L for model 2 is changed to 1.288L so the value of LL for model 2 becomes to the same as the value of L for model 1. The heat loss from the model 1 is almost the same that from the model 2 for given range of L. Precisely, the heat loss from the model 2 is slightly less than that from the model 1 until L = 2.5 and vice versa over L = 2.5. Figure 8 presents the same type of information as Fig. 7 except Bi = 0.1. In case of Bi = 0.1, the values of the heat loss increase almost linearly as L increases while those values increase somewhat parabolically as L increases for Bi = 0.01. This figure shows the heat loss from the model 1 is greater than that from the model 2 for given range of L and the difference between two values is diminish as L increases. Finally, last two figures show that the heat loss does not change remarkably as the model 1 changes to the model 2 for given range of Biot number and the non-dimensional fin length.

4. Conclusion

The relative error of the heat loss between analytical method and finite difference method for the fin model 2 diminishes considerably as comparing that for the fin model 1 for given range of the non-dimensional fin length and Biot number. These results seem to be due to the proper setting up the nodes for the fin model 2 when the finite difference method is used. So it seems to be that more exact results can be obtained if nodes are set up properly and the number of nodes increases in the case of using the finite difference method. Finally, even though the shape of the fin changed from the parabolic fin whose parabolic curves meet at the fin center line to the fin whose fin tip cuts vertically at the ratio LL = 0.776L, the value of the heat loss calculated by using the two-dimensional analytical method does not change remarkably for given range of Biot number and the non-dimensional fin length.

References

[1] Lee, S. C., Park, B. D., Lee, J. H. and Han, W. H., "Condensation and Evaporation Heat Transfer Characteristics of HFC-134a in a Horizontal Smooth and a Micro-finned Tube", *KSME(B)*, Vol. 20, No. 5, pp. 1724 1734.

[2] Kang, H. C. and Kim, M. H., "A Large Scale Model Test to Investigate the Pressure Drop and Heat Transfer Characteristics in the Air Side of Two-Row Heat Exchanger", *KSME(B)*, Vol. 21, No. 1, pp. 113 124.

[3] Kraus, A. D. and Snider, A. D. and Doty, L. F., 1978, "An efficient Algorithm for Evaluating Arrays of Extended Surface, " *ASME J. of Heat Trans.*, Vol. 100, pp. 288 293.

[4] Ünal, H. C., 1987, "Temperature Distributions in Fins with Uniform and Non-Uniform Heat Generation and Non-Uniform Heat Transfer Coefficient, " *Int. J. Heat and Mass Trans.*, Vol. 30, pp. 1465 1477.

[5] Sen, A. K. and Trinh, S., 1986, "An Exact Solution for The Rate of Heat Transfer From a Rectangular Fin Governed by a Power Law-Type Temperature Dependence, " *ASME J. of Heat Trans.*, Vol. 108, pp. 457 459.

[6] Suryanarayana, N. V., 1977, "Two-Dimensional Effects on Heat Transfer Rates From an Array of Straight Fins, " *ASME J. of Heat Trans.*, Vol. 99, pp. 129 132.

[7] Look, Jr., D. C., 1989, "Two-Dimensional Fin with Non-Constant Root Temperature, " *Int. J. of Heat and Mass Trans.*, Vol. 32, pp. 977 980.

[8] Kang, H. S., 1997, "Comparison of Performances of the Various Shapes of Asymmetric Fins, " *KSME International Journal*, Vol. 11, No. 3, pp. 311 318.

[9] Beck, J. V. and Litkouhi, B., 1988, "Heat Conduction Numbering System for Basic Geometries, " *Int. J. of Heat and Mass Trans.*, Vol. 31, pp. 505 515.

[10] Al-Najem, N. M. and Özisik, M. N., 1985, "On the solution of Three-Dimensional Inverse Heat Conduction in Finite Media, " *Int. J. of Heat and Mass Trans.*, Vol. 28, pp. 2121 2128.7

[11] Kang, H. S. and Look, Jr., D. C., 1997, "Two Dimensional Trapezoidal Fins Analysis, " *Computational Mechanics*, Vol. 19, No. 3, pp. 247 250.

[12] Ullmann, A. and Kalman, H., 1989, "Efficiency and Optimized Dimensions of Annular Fins of Different Cross-Section Shapes, " *Int. J. of Heat and Mass Trans.*, Vol. 32, pp. 1105 1110.

[13] Brown, A., 1965, "Optimum Dimensions of Uniform Annular Fins, " *Int. J. of Heat and Mass Trans.*, Vol. 8, pp. 655 662.

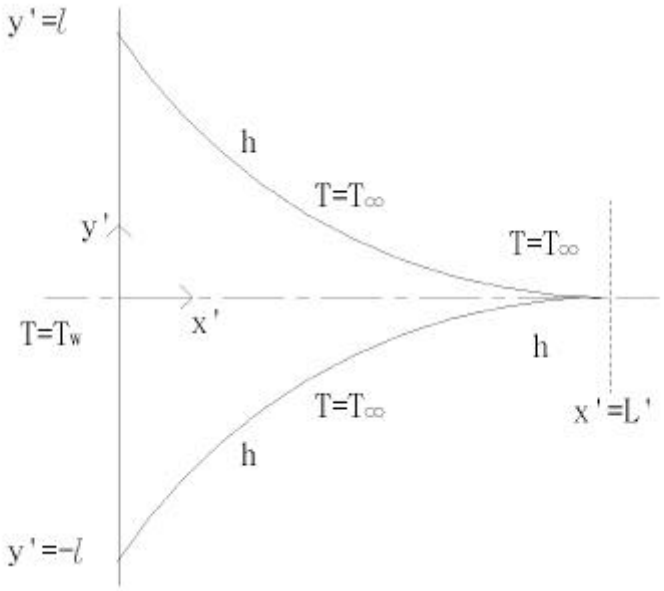

Fig. 1-a Geometry of a parabolic fin (model 1)

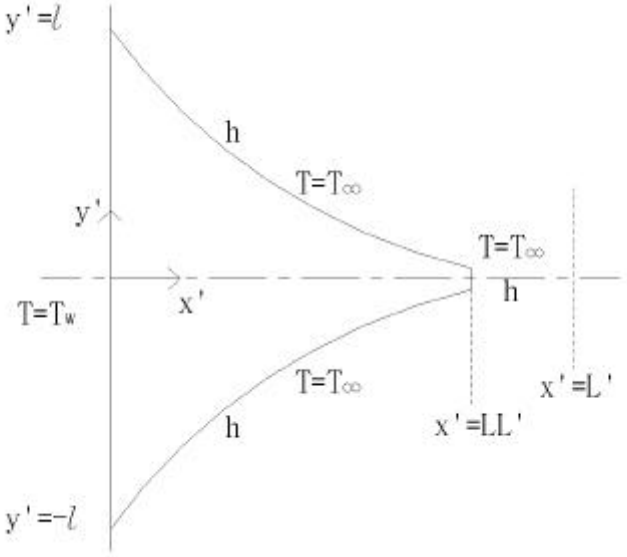

Fig. 1-b Geometry of a parabolic fin whose tip is cut (model 2)

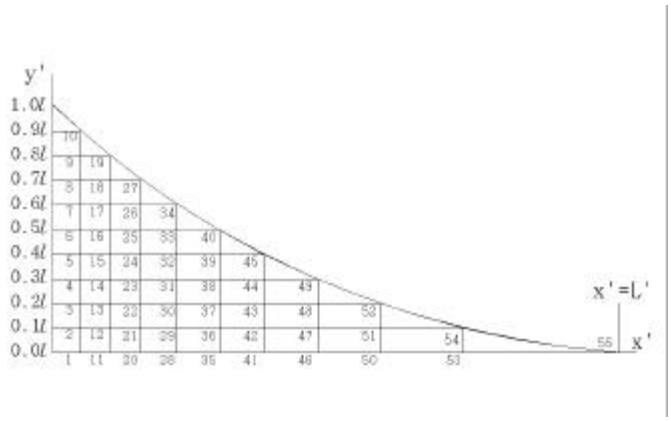

Fig. 2-a Upper half fin geometries presenting 55nodes for model 1

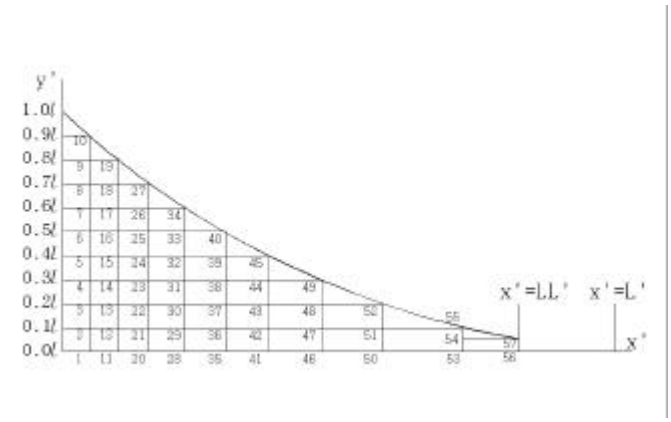

Fig. 2-b Upper half fin geometries presenting 57 nodes for model 2

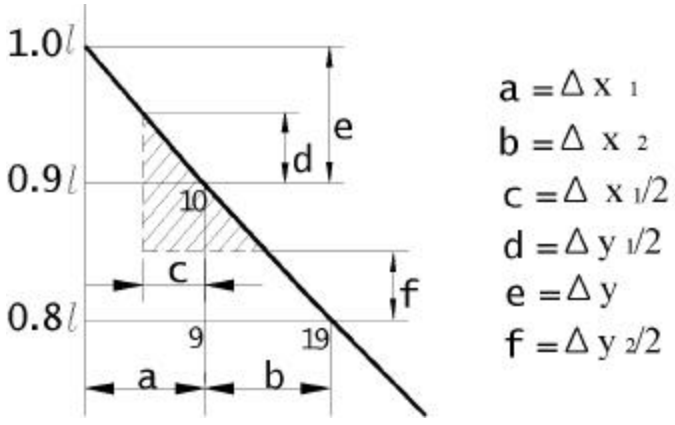

Fig. 2-c The definition of notation for a finite difference method

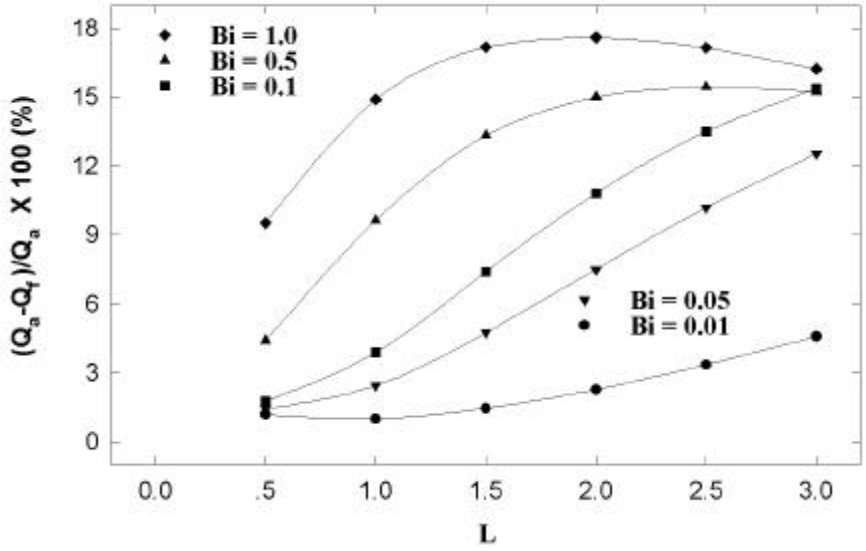

FIG. 3 Relative error of the heat loss versus the non-dimensional fin length for model 1

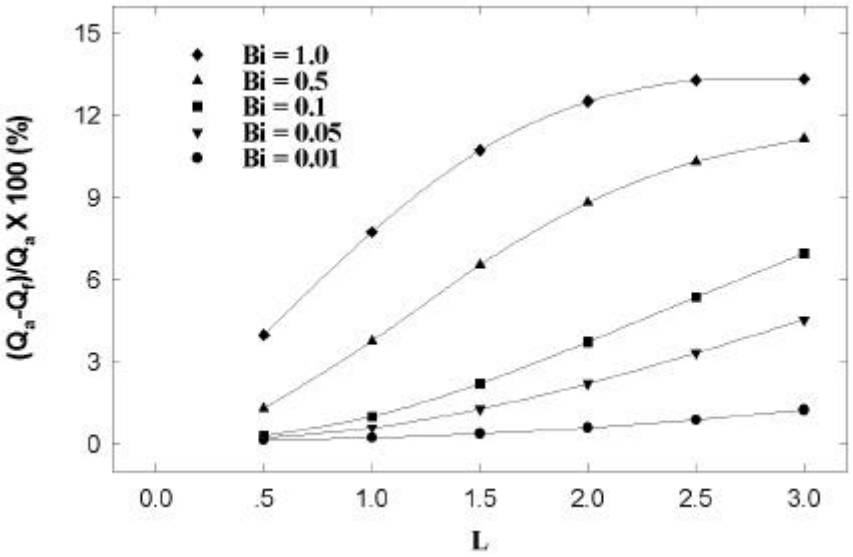

Fig. 4 Relative error of the heat loss versus the non-dimensional fin length for model 2

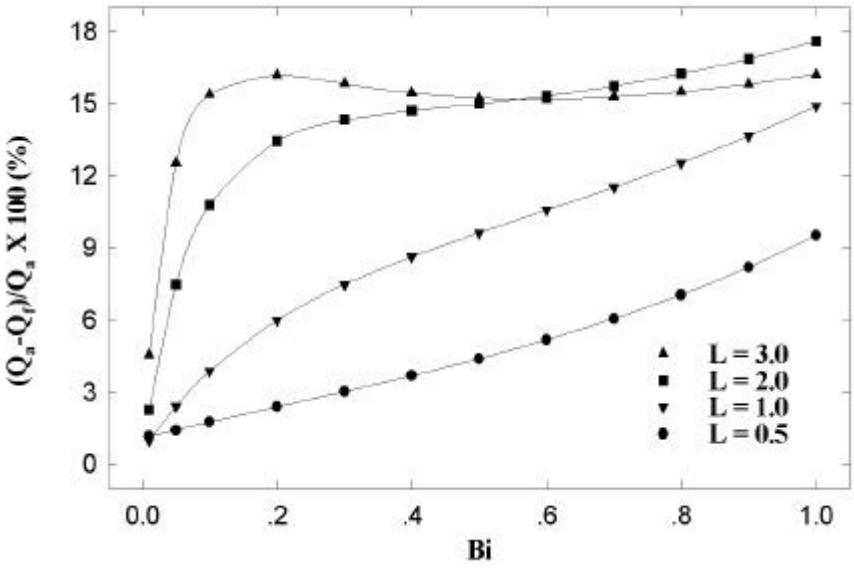

Fig.5 Relative error of the heat loss versus the Biot number for model 1

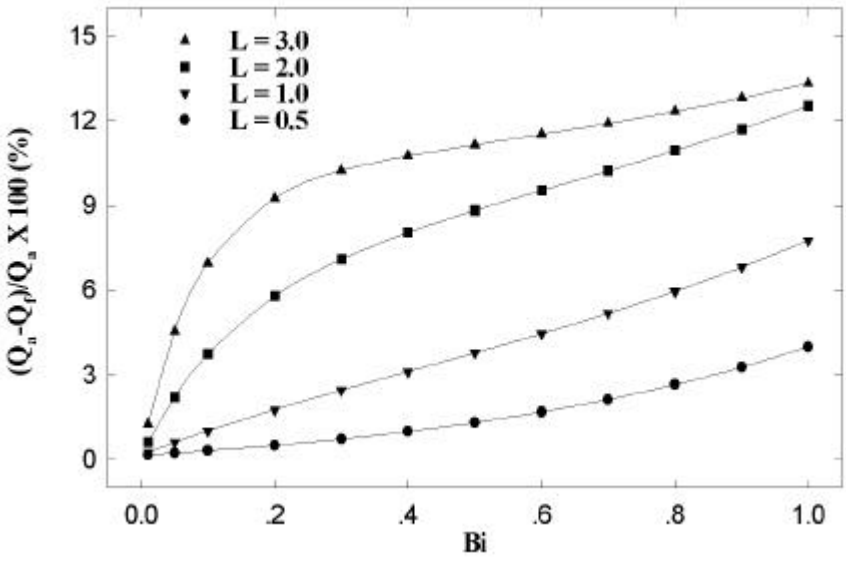

Fig. 6 Relative error of the heat loss versus the Biot number for model 2

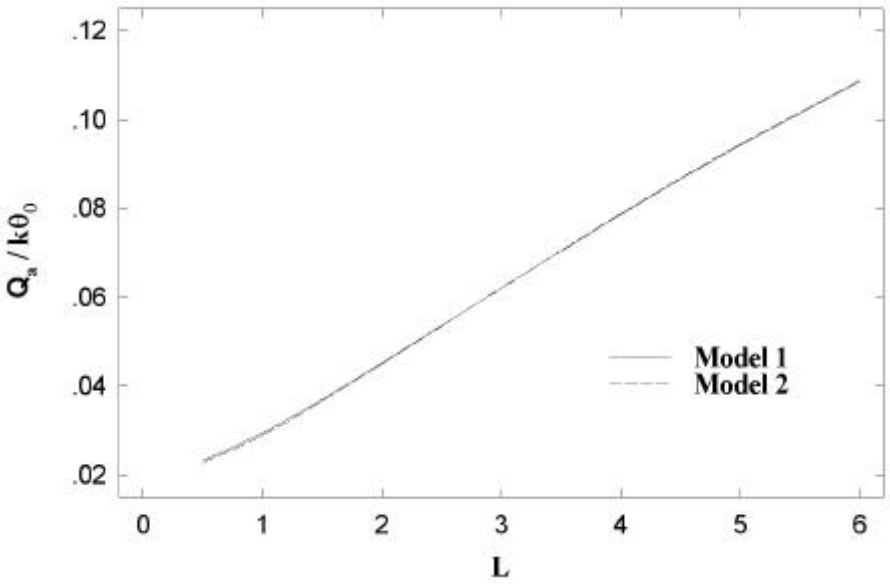

Fig. 7 The heat loss obtained by using the analytical method versus the non-dimensional fin length for Bi=0.01

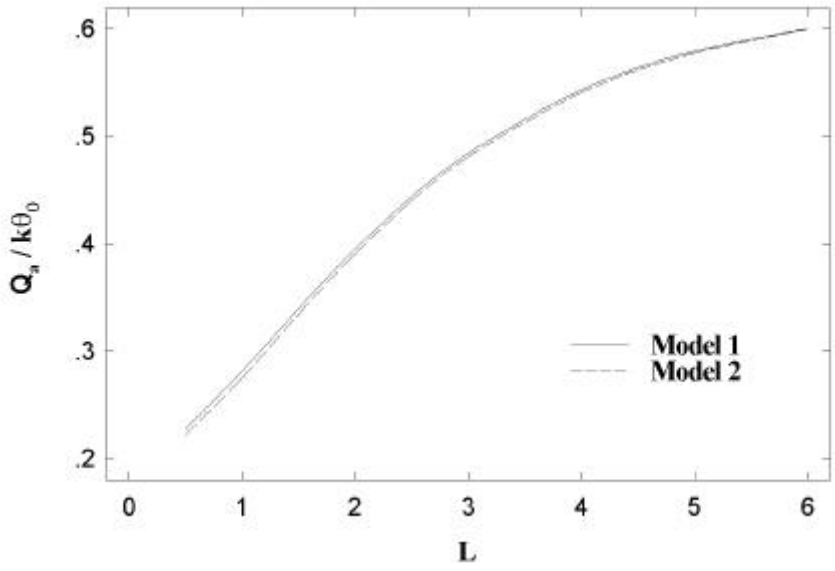

Fig. 8 The heat loss obtained by using the analytical method versus the non-dimensional fin length for Bi=0.1